2024 IEEE 63rd Conference on Decision and Control (CDC)
December 16-19, 2024. MiCo, Milan, Italy

A Model Predictive Control Approach for Smooth Traffic Flow of Connected Autonomous Vehicles at Signalized Junctions

Rudra Sen, *Student Member, IEEE* and Subashish Datta, *Member, IEEE*

***Abstract*— In this article, we consider the problem of controlling a group of autonomous vehicles, which are maneuvering on a road, such that smooth traffic flow can happen. For this, we propose that every autonomous vehicle maneuvers with a pre-specified velocity profile. The velocity profiles are determined in such a way that either none of the vehicles wait near a signalized junction or only a limited number of vehicles are accumulated when the red light is ON. To maneuver the autonomous vehicles with a pre-specified velocity profile, a control sequence is generated using a receding horizon control approach in the model-predictive control framework. The associated problems, such as the feasibility of the underlying constrained optimization problem at every stage and the convergence analysis, are also considered. The efficacy of the proposed approach is evinced with numerical simulations.**

***Index Terms*— Autonomous vehicles, Traffic control, Model predictive control, LMI.**

I. Introduction

Nowadays, traffic congestion has emerged as a major issue in urban areas due to the growing population and increased transportation needs. Some of the important factors in urban transportation systems that need special attention are smooth traffic flow, reduction in traffic congestion, avoidance of accidents, and reduction in waiting time at signal posts. At present, the most commonly adopted methodology to manage roadway traffic flow at a signalized junction (SJ) is through *traffic signals*. It has been observed in roadway traffic that drivers maneuver their vehicles with maximum possible velocities to reduce the travel time for reaching their destinations. This maneuvering raises the risk of accidents and causes vehicle congestion near SJs. Due to the fixed duration of the green light ON near a SJ, only a limited number of vehicles can cross, while others need to wait until the next green signal turns on. This increases unnecessary wait-time for the commuters near SJs, causing travel weariness. TomTom Traffic Index 2023 [1] indicates that the extra travel time required in major cities in India such as Bangalore, New Delhi, and Mumbai are 63%, 48%, and 43%, respectively, in comparison to free-flow traffic conditions.

To address the aforementioned issues, in this work, we propose a scenario where every vehicle maneuvers with a *pre-specified reference velocity profile* on roadway traffic. The velocity profile for a vehicle is determined in such a way that either none of the vehicles wait at an SJ or only a limited number of vehicles get accumulated at an SJ when the red light is ON. Our approach assumes a simple roadway traffic scenario with only autonomous vehicles (AVs), and there are provisions for vehicle-to-infrastructure (V2I) and vehicle-to-vehicle (V2V) communications. Further, the AVs are identical, and they are maneuvering on a single lane through multiple signalized junctions. Additionally, it is assumed that each AV has its own sensing equipment and local controllers to generate appropriate control signals. We consider a linear time-invariant continuous time model for each AV. After performing discretization of the model using the *zero-order hold* method, we use the *receding horizon control* (RHC) approach in the model-predictive control (MPC) framework to generate appropriate control signals for each AV. By designing suitable online *polyhedral terminal set* for each AV, the inherent important issues in the RHC approach, such as *recursive feasibility* and *stability*, are addressed.

The platoon control method for AVs has drawn significant attention from researchers to address traffic congestion related issues. To deal with traffic congestion at the unsignalized junctions, an intersection manager-based centralized coordination framework is proposed in [2] for scheduling the AVs appropriately. Some of the other scheduling strategies for AVs at unsignalized junctions include graph-based AV scheduling approaches [3], bilevel energy-optimal coordination framework [4], time-optimal control framework [5], MPC framework [6]–[9]. Similarly, several control approaches, such as multi-intersections-based fuel efficient predictive control strategy [10], optimal control framework [11], MPC framework [12]–[15] and adaptive dynamic programming approach [16] are proposed to reduce traffic congestion at signalized junctions. In the existing MPC-based control approaches, however, the issues related to recursive feasibility and stability are not investigated.

Notation: $x^i_{j|k}$ refers the predicted value of x of i^{th} AV at time step $(k+j)$ having the information at step k; $S \succ 0$ denotes that S is symmetric positive definite matrix. $\|p\|^2_S := p^\mathsf{T} S p$ is weighted 2-norm of a vector p with weight matrix S. I_q denotes the identity matrix of size $q \times q$. $\mathbb{I}^b_a$ denotes the set of integers in the interval $[a, b]$. *m/sec* and *sec* refer to meter/sec and sec, respectively.

II. Main Results

We consider a platoon of autonomous vehicles traveling on a roadway in a single lane. The first AV, which enters into the control zone of a roadway, is considered as *leader*, and other AVs are considered as *followers*. The set of such AVs is referred to as *connected autonomous vehicles* (CAVs). In this section, we first briefly describe the considered dynamics for

Rudra Sen and Subashish Datta are with the Department of Electrical Engineering, Indian Institute of Technology Delhi, New Delhi 110016, India. rudra.sen@ee.iitd.ac.in, subashish@ee.iitd.ac.in

979-8-3503-1632-2/24/$31.00 ©2024 IEEE

an AV and, thereafter, propose methods for providing control signals to ensure smooth traffic flow at signalized crossings.

Since each AV is traveling one after the other in a single lane, we only consider the longitudinal motion of the vehicles, and their lateral dynamics are ignored. The following linearized model for longitudinal motion of i^{th} AV is considered (refer to [17], [18] for more details):

$$\underbrace{\begin{bmatrix}\dot{p}^i(t)\\ \dot{v}^i(t)\\ \dot{a}^i(t)\end{bmatrix}}_{\dot{x}^i(t)} = \underbrace{\begin{bmatrix}0 & 1 & 0\\ 0 & 0 & 1\\ 0 & 0 & -\frac{1}{\eta_i}\end{bmatrix}}_{A} \underbrace{\begin{bmatrix}p^i(t)\\ v^i(t)\\ a^i(t)\end{bmatrix}}_{x^i(t)} + \underbrace{\begin{bmatrix}0\\ 0\\ \frac{1}{\eta_i}\end{bmatrix}}_{B} u^i(t). \tag{1}$$

where p^i, v^i, and a^i denote the position, velocity, and acceleration of i^{th} AV, respectively, η_i denotes the engine time constant, and the control input $u^i \in \mathbb{R}$ represents the throttle input to i^{th} AV engine. We discretize (1) using the *zero-order hold* method as in [19, Chapter 3] with sampling time t_s, and is represented as follows:

$$\underbrace{\begin{bmatrix}p^i_{k+1}\\ v^i_{k+1}\\ a^i_{k+1}\end{bmatrix}}_{x^i_{k+1}} = \underbrace{\begin{bmatrix}1 & t_s & \eta_i^2 e^{-\frac{t_s}{\eta_i}} + \eta_i t_s - \eta_i^2\\ 0 & 1 & \eta_i - \eta_i e^{-\frac{t_s}{\eta_i}}\\ 0 & 0 & e^{-\frac{t_s}{\eta_i}}\end{bmatrix}}_{A_d} \underbrace{\begin{bmatrix}p^i_k\\ v^i_k\\ a^i_k\end{bmatrix}}_{x^i_k} + \underbrace{\begin{bmatrix}b_1\\ b_2\\ b_3\end{bmatrix}}_{B_d} u^i_k. \tag{2}$$

where $b_1 = t_s^2/2 - \eta_i^2(e^{-\frac{t_s}{\eta_i}} - 1) - \eta_i t_s$, $b_2 = t_s + \eta_i(e^{-\frac{t_s}{\eta_i}} - 1)$, and $b_3 = 1 - e^{-\frac{t_s}{\eta_i}}$. The velocity v^i_k, acceleration a^i_k, and control input u^i_k of each AV are considered to be bounded by their upper and lower limits as follows:

$$\underline{v} \le v^i_k \le \overline{v}, \quad \underline{a} \le a^i_k \le \overline{a}, \quad \underline{u} \le u^i_k \le \overline{u}. \tag{3}$$

where $\underline{v}$, $\underline{a}$, and $\underline{u}$ denote the *minimum* values of velocity, acceleration, and control input respectively, and $\overline{v}$, $\overline{a}$, and $\overline{u}$ denote the *maximum* values of velocity, acceleration, and control input respectively. Further, to ensure the avoidance of rear-end collision between vehicle i and the preceding vehicle l, we assume that a safe distance is maintained between them. Such safe distance is modeled as follows:

$$p^l_k - p^i_k \ge \gamma + \rho v^i_k, \tag{4}$$

where γ is the static gap, and ρ is the reaction time.

As introduced in Section I, we first need to generate a reference velocity profile for each AV. Considering the velocity constraints in (3), we now propose an algorithm, similar to [12], [16], for generating such reference velocity.

A. Generation of Reference Velocity for AVs

Assume that each SJ has its own control zone. Once an AV enters into this control zone, it can access the traffic signal duration information of that SJ. At each SJ, the time period for which the red signal will remain ON is referred to as *red-time* τ_r. Similarly, the time period for which the green signal will remain ON is referred to as *green-time* τ_g. Let d_m be the distance from the AV's position to the upcoming SJ, denoted as SJ_m. Assume that SJ_m broadcasts the following information to a vehicle once it enters into the control zone: (i) the time period τ_0, after which the next signal, either green or red, will become ON, and (ii) the duration of red time τ_r and green-time τ_g. Considering this information as inputs to an AV, we now propose a procedure in Algorithm 1 to generate reference velocity for that AV. In order to generate the signal sequence as explained in Algorithm 1, each AV communicates with SJs through V2I communication within the control zone. Further, each AV communicates exclusively through a V2V connection with its preceding vehicle to ensure collision-free maneuvering. In this way, there is no exchange of information among AVs through any centralized command unit.

Explanation for Algorithm 1: *Steps 1-7:* A sequence of time periods is generated based on the information (τ_0, τ_g, τ_r, and whether the red or green light turns ON after τ_0 sec) received from m^{th} signalized junction SJ_m. In steps 1 to 3, we compute: $\tau_{r_1} = \tau_0 + \tau_g$, $\tau_{g_2} = \tau_{r_1} + \tau_r$ up-to Γ, and generate a sequence $\mathcal{N}$, if the green signal turns ON after τ_0 sec. The time horizon Γ is chosen to be large enough (possibly: $\Gamma \ge 2(\tau_0 + \tau_r + \tau_g)$) so that each AV gets a feasible green interval to cross SJ_m. Similarly, in steps 4 to 6, we compute $\tau_{g_2} = \tau_0 + \tau_r$, $\tau_{r_2} = \tau_{g_2} + \tau_g$ up-to Γ, and generate a sequence $\mathcal{N}$, if the red signal turns ON after τ_0 sec. For instance, let SJ_m broadcasts: $\tau_0 = 20$ sec, $\tau_g = 20$ sec, and $\tau_r = 25$ sec, and the green signal turns ON after τ_0 sec. Then, by selecting $\Gamma = 175$ sec, the generated signal sequence is: $\mathcal{N} = \{20, 40, 65, 85, 110, \ldots, 175\}$, as shown in Fig. (1).

Algorithm 1 Generation of Reference velocity (v_{ref})

```
Input: $d_m$, $[\underline{v}, \overline{v}]$, $\delta$, $\tau_0$, $\tau_g$, $\tau_r$
Output: $v_{ref}$
 1: if green signal ON after $\tau_0$ then
 2:     $\tau_{r_1} \leftarrow (\tau_0 + \tau_g)$, $\tau_{g_2} \leftarrow (\tau_{r_1} + \tau_r)$, ...up-to $\Gamma$
 3:     $\mathcal{N} \leftarrow \{\tau_0, \tau_{r_1}, \tau_{g_2}, \ldots$ up-to $\Gamma\}$
 4: else if red signal ON after $\tau_0$ then
 5:     $\tau_{g_2} \leftarrow (\tau_0 + \tau_r)$, $\tau_{r_2} \leftarrow (\tau_{g_2} + \tau_g)$...up-to $\Gamma$
 6:     $\mathcal{N} \leftarrow \{\tau_0, \tau_{g_2}, \tau_{r_2}, \ldots$ up-to $\Gamma\}$
 7: end if
 8: for $j$ = 1 : length($\mathcal{N}$) do
 9:     $V_{feasible} \leftarrow \left[\frac{d_m}{\tau_{r_j} - \delta}, \frac{d_m}{\tau_{g_j} + \delta}\right] \cap [\underline{v}, \overline{v}]$
10:     if ($V_{feasible} \neq \emptyset$) then
11:         $[v_{low}, v_{high}] \leftarrow V_{feasible}$
12:         break
13:     else continue
14:     end if
15: end for
16: return $v_{ref} \leftarrow v_{high}$
```

Steps 8-13: In these steps, we compute the reference velocity profile for an AV to cross SJ_m. Let d_m be the distance from the AV's position to the upcoming signalized junction SJ_m. Adding a certain level of safety margin, let the j^{th} green light interval (as shown in Fig. (1)) be: $[\tau_{g_j} + \delta, \tau_{r_j} - \delta]$ (instead of $[\tau_{g_j}, \tau_{r_j}]$), where δ is some small positive number. Then, by considering the velocity constraint for an AV, we compute the velocity interval as follows: $V_{feasible} = \left[\frac{d_m}{\tau_{r_j} - \delta}, \frac{d_m}{\tau_{g_j} + \delta}\right] \cap [\underline{v}, \overline{v}]$. If we get a feasible velocity interval: $V_{feasible} \neq \emptyset$, then the highest value of $V_{feasible}$; that is, v_{high} is considered as reference velocity v_{ref} for an AV; else the AV will compute the velocity interval $V_{feasible}$ for $(j+1)^{th}$ green light interval: $[\tau_{g_{j+1}} + \delta,\ \tau_{r_{j+1}} - \delta]$. For instance, by considering $d_m = 1000$ m, $\delta = 5$ sec, $\underline{v} = 0$ m/sec, and $\overline{v} = 25$ m/sec, the feasible velocity interval for 1^{st} green light interval be computed as: $V_{feasible} = [28.57, 40] \cap [0, 25] = \emptyset$. Therefore, the search is continued for the 2^{nd} green light interval, where a feasible velocity interval is obtained as follows: $V_{feasible} = [12.5, 14.28] \cap [0, 25] = [12.5, 14.28]$. Hence, the reference velocity of the AV is $v_{ref} = 14.28$ m/sec. This is demonstrated in Fig. (1).

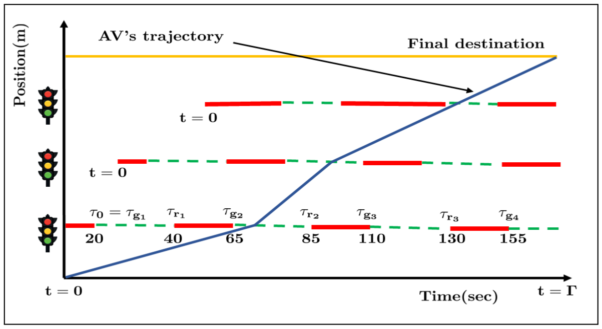

Fig. 1. Schematic of the trajectory of an AV, passing through three SJs. Red (solid) and green (dashed) lines denote the red signal and green signal turn-ON timings, respectively. The j^{th} green light interval is: $[\tau_{g_j} + \delta, \tau_{r_j} - \delta]$.

B. Control Scheme for an AV

Once v_{ref} is generated for an AV using Algorithm 1, it is required to accelerate/decelerate the vehicle through an appropriate control scheme to reach that velocity profile. Since the states and control signals are constrained to satisfy (3) and (4), an acceptable control signal (sequence of signals) is computed by solving a constrained optimization problem in the MPC framework [20]. For this, we considered a nonzero steady-state reference point $x^i_{ref} = [p^i_{ref}, v^i_{ref}, 0]^\top$ for an i^{th} AV. With respect to the vehicle dynamics as in (2), at steady state, we have: $x^i_{k+1} = x^i_k = x^i_{ref}$. Then, by denoting u^i_{ref} as input to the vehicle at steady state, we obtain the following relation from (2):

$$x^i_{ref} = A_d x^i_{ref} + B_d u^i_{ref} \Rightarrow B_d u^i_{ref} = (I_n - A_d) x^i_{ref}. \quad (5)$$

Note that in the expression (5), it may not be possible to compute u^i_{ref} exactly for every given x^i_{ref}. In that case, we consider u^i_{ref} as a minimum-norm solution to an associated least-squares problem, and the solution is computed as follows: $u^i_{ref} = B^\dagger_d (I_n - A_d) x^i_{ref}$, where $B^\dagger_d$ is the pseudo-inverse of B_d. Then, by considering x^i_{ref} and u^i_{ref}, we formulate the quadratic reference tracking cost function J^i_k for our optimization as follows: $J^i_k = \|x^i_{j|k} - x^i_{ref}\|^2_Q + \|u^i_{j|k} - u^i_{ref}\|^2_R$, where $Q \succeq 0$ and $R = B^T_d W B_d > 0$ (with W is a positive scalar) are the state and control input weight matrices, respectively. Further, we also include a terminal cost $\|x^i_{N|k} - x^i_{ref}\|^2_P$ to the cost function J^i_k, where $P \succ 0$ is terminal cost weight matrix and N is the prediction horizon. After the end of prediction horizon N, it is expected that the state $x^i_{N|k}$ should reach a pre-defined terminal set $\mathcal{X}^i_{\mathcal{T}_k}$; that is, $x^i_{N|k} \in \mathcal{X}^i_{\mathcal{T}_k}$. In the MPC setting, we need the terminal set $\mathcal{X}^i_{\mathcal{T}_k}$ to be a *maximal positive invariant set*. We now give a procedure to construct the set $\mathcal{X}^i_{\mathcal{T}_k}$.

Consider the vehicle dynamics (2). Assume that a control law: $u^i_k = u^i_{ref} + K(x^i_k - x^i_{ref})$, where K is feedback gain matrix, is applied to i^{th} AV only within the terminal set $\mathcal{X}^i_{\mathcal{T}_k}$. Hence, the closed-loop system inside $\mathcal{X}^i_{\mathcal{T}}$ is:

$$x^i_{k+1} = (A_d + B_d K) x^i_k + B_d (u^i_{ref} - K x^i_{ref}), \quad (6)$$

It follows from (5) that $B_d u^i_{ref} = (I_n - A_d) x^i_{ref}$. Using this relation in (6), we have the following autonomous system inside the terminal set $\mathcal{X}^i_{\mathcal{T}_k}$:

$$x^i_{k+1} = (A_d + B_d K) x^i_k + (I_n - (A_d + B_d K)) x^i_{ref}. \quad (7)$$

Let the constraint sets given in (3) and (4) be written in the following form:

$$F^i x^i_k \leq \xi^i_k, \quad g^i u^i_k \leq \beta^i. \quad (8)$$

where

$$F^i = \begin{bmatrix} 1 & \rho & 0 \\ 0 & 1 & 0 \\ 0 & 0 & 1 \\ 0 & -1 & 0 \\ 0 & 0 & -1 \\ 0 & 0 & 0 \\ 0 & 0 & 0 \end{bmatrix}, \ g^i = \begin{bmatrix} 0 \\ 0 \\ 0 \\ 0 \\ 0 \\ 1 \\ -1 \end{bmatrix}, \ \xi^i_k = \begin{bmatrix} p^l_{j|k} - \gamma \\ \overline{v} \\ \overline{a} \\ -\underline{v} \\ -\underline{a} \\ 0 \\ 0 \end{bmatrix}, \ \beta^i = \begin{bmatrix} 0 \\ 0 \\ 0 \\ 0 \\ 0 \\ \overline{u} \\ -\underline{u} \end{bmatrix}.$$

Now, by adding both the equations in (8), and replacing $u^i_k = u^i_{ref} + K(x^i_k - x^i_{ref})$, we have the following relation:

$$(F^i + g^i K) x^i_k \leq \xi^i_k + \beta^i + g^i (K x^i_{ref} - u^i_{ref}). \quad (9)$$

Note that the inequality (9) becomes a constraint set for the closed-loop dynamics (7) inside the terminal set $\mathcal{X}^i_{\mathcal{T}_k}$. Using (9), define a constraint set for closed-loop dynamics (7) as:

$$\Omega^i_k = \{x^i_k : (F^i + g^i K) x^i_k \leq c^i_k, \forall x^i_k \in \mathcal{X}^i_{\mathcal{T}_k}\}. \quad (10)$$

where $c^i_k = \xi^i_k + \beta^i + g^i (K x^i_{ref} - u^i_{ref})$. Then, it follows from [20, Theorem 10.1] that the terminal set $\mathcal{X}^i_{\mathcal{T}_k}$ is a maximal positive invariant set with respect to the closed-loop dynamics (7) with constraint set (10) if and only if:

$$\mathcal{X}^i_{\mathcal{T}_k} \subseteq Pre(\mathcal{X}^i_{\mathcal{T}_k}) \quad (11)$$

where $Pre(\mathcal{X}^i_{\mathcal{T}_k})$ is the *precursor set* of $\mathcal{X}^i_{\mathcal{T}_k}$ [20, Chapter 10]. The relation (11) implies $Pre(\mathcal{X}^i_{\mathcal{T}_k}) \cap \mathcal{X}^i_{\mathcal{T}_k} = \mathcal{X}^i_{\mathcal{T}_k}$. Using this, we now propose Algorithm 2 to compute $\mathcal{X}^i_{\mathcal{T}_k}$.

Algorithm 2 Computation of $\mathcal{X}^i_{\mathcal{T}_k}$ for i^{th} AV [20, Chapter 10]

```
Input: System dynamics (7), Constraint set $\Omega^i_k$ as in (10)
Output: Maximal positive invariant set $\mathcal{X}^i_{\mathcal{T}_k}$
$\Psi_0 \leftarrow \Omega^i_k$, $l \leftarrow 0$
while (1) do
    $\Psi_{l+1} \leftarrow Pre(\Psi_l) \cap \Psi_l$
    if ($\Psi_{l+1} = \Psi_l$) then break
    else
        $\Psi_l \leftarrow \Psi_{l+1}$
    end if
    $l \leftarrow l + 1$
end while
return $\mathcal{X}^i_{\mathcal{T}_k} \leftarrow \Psi_l$
```

Once, the maximal positive invariant sets $\mathcal{X}^i_{\mathcal{T}_k}$ are computed using Algorithm 2, we use them to formulate the following constrained optimization problem $\mathbb{OP}$:

$$\mathbb{OP}: \min_{U^i_k \in \mathcal{U}^i} J^i_k \triangleq \|x^i_{N|k} - x^i_{ref}\|^2_P + \sum_{j=0}^{N-1}\left\{\|x^i_{j|k} - x^i_{ref}\|^2_Q + \|u^i_{j|k} - u^i_{ref}\|^2_R\right\} \quad \text{(12a)}$$

$$\text{subject to, } \; x^i_{j+1|k} = A_d x^i_{j|k} + B_d u^i_{j|k}, \;\; \forall j \in \mathbb{I}_0^{N-1} \quad \text{(12b)}$$

$$x^i_{0|k} = x^i_k, \;\; F^i x^i_{j|k} \le \xi^i_k, \;\; g^i u^i_{j|k} \le \beta^i, \;\; \forall j \in \mathbb{I}_0^{N-1} \quad \text{(12c)}$$

$$x^i_{N|k} \in \mathcal{X}^i_{\mathcal{T}_k}, \quad \text{(12d)}$$

where $\mathcal{U}^i$ is input constraint set. To obtain a sequence of control inputs for i^{th} AV, we use the RHC approach in the MPC framework, where the optimization $\mathbb{OP}$ needs to be solved repeatedly at each time step over the prediction horizon N. There is a possibility that the optimization $\mathbb{OP}$ becomes infeasible at some time step. In the following result, we show that the imposition of constraint (12d) will ensure that the feasibility of $\mathbb{OP}$ at the first step guarantees the feasibility of $\mathbb{OP}$ at every step.

Lemma 1: Assume that the state vector $x^i_{N|k} \in \mathcal{X}^i_{\mathcal{T}_k}$. Let the optimization $\mathbb{OP}$ be feasible at time step k. Then, $\mathbb{OP}$ is feasible for future time step: $k + j$, $\forall j \in \mathbb{I}_0^{\infty}$.

Proof: Given that the optimization $\mathbb{OP}$ is feasible at time step k (it satisfies (12b), (12c) and (12d)), there exists an optimal control sequence $U^i_k = \{u^i_{j|k}\}_{j=0}^{N-1}$. Let the corresponding optimal state sequence be: $X^i_k = \{x^i_{j|k}\}_{j=0}^{N}$, which satisfies the state and input constraints (12c) and the terminal constraint $x^i_{N|k} \in \mathcal{X}^i_{\mathcal{T}_k}$. For the time step $k+1$, construct a control sequence as follows:

$$\widetilde{U}^i_{k+1} = \{u^i_{1|k}, u^i_{2|k}, u^i_{3|k} \cdots, u^i_{N-1|k}, u^i_{N-1|k+1}\} \quad (13)$$

where $\{u^i_{j|k}\}_{j=1}^{N-1}$ are the optimal control sequence computed at time-step k and $u^i_{N-1|k+1} := u^i_{ref} + K(x^i_{N|k} - x^i_{ref})$. Note that the choice of last control sequence $u^i_{N-1|k+1}$ is possible, since at k^{th} time-step: $x^i_{N|k} \in \mathcal{X}^i_{\mathcal{T}_k}$. Then, the corresponding predicted state sequence be: $\widetilde{X}^i_{k+1} = \{x^i_{j|k+1}\}_{j=0}^{N}$, where $x^i_{j|k+1} = x^i_{j+1|k}$, $\forall j \in \mathbb{I}_0^{N-1}$ and $x^i_{N|k+1} = A_d x^i_{N|k} + B_d(u^i_{ref} + K(x^i_{N|k} - x^i_{ref}))$. The last state vector is the same as in (6) since it is inside the terminal set $\mathcal{X}^i_{\mathcal{T}_k}$. This shows that the optimization problem $\mathbb{OP}$ has a feasible solution at $k+1$ time-step. Note that the constructed control sequence (13) may not be an optimal control sequence. However, it guarantees the feasibility of $\mathbb{OP}$. Hence, in a similar way, we can extend the control sequence construction process for $(k+j)^{th}$ steps for $j \in \mathbb{I}_0^{\infty}$. This is possible due to the fact that $x^i_{N|k+j} \in \mathcal{X}^i_{\mathcal{T}_k}$. Hence, the feasibility of $\mathbb{OP}$ is ensured at every time step. ■

Note that according to Lemma 1, the feasibility of $\mathbb{OP}$ at k^{th} time step guarantees that it is feasible for all future time steps. We now give a procedure to select the initial states $x^i_{0|0}$ such that the optimization is feasible at time step $k = 0$. For this, we first construct a set $\mathcal{X}^i_0$ as follows, which is the *N-step backward reachable set* to terminal set $\mathcal{X}^i_{\mathcal{T}_k}$ [20, see definition in Chapter 10]. First, consider the the terminal set $\mathcal{X}^i_{\mathcal{T}_k}$, and define $\mathcal{S}_N = \mathcal{X}^i_{\mathcal{T}_k}$. Compute $\mathcal{S}_{N-1} = Pre(\mathcal{S}_N) \cap \mathcal{X}^i$, where $\mathcal{X}^i = \{x^i_k : F^i x^i_k \le \xi^i_k\}$. Continue this process until $N = 0$. Then, the resulting set $\mathcal{X}^i_0$ is *N-step backward reachable set* of $\mathcal{X}^i_{\mathcal{T}_k}$. Note that the sets $\mathcal{X}^i_{\mathcal{T}_k}$, $Pre(\mathcal{X}^i_{\mathcal{T}_k})$, $\mathcal{X}^i_0$ are polyhedral sets, which are characterized by a set of linear inequalities. To construct all such sets, one may use the Multi-Parametric Toolbox (MPT) [21] in MATLAB.

We now show that the state trajectory $x^i_{j|k}$, generated by the application of control sequence U^i_k according to the RHC approach, converges to the reference state trajectory x^i_{ref}. This is ensured by appropriately designing the terminal cost matrix P and feedback gain matrix K.

Lemma 2: Let the cost functions of $\mathbb{OP}$ at time steps k and $k+1$ be J^i_k and J^i_{k+1}, respectively. Assume that $\mathbb{OP}$ is feasible at time step k. Then, the following relation holds: $J^i_{k+1} \le J^i_k$, $k = 0, 1, 2, \cdots$, if

$$(A_d + B_d K)^{\mathsf{T}} P (A_d + B_d K) - P + Q + K^{\mathsf{T}} R K \preceq 0. \quad (14)$$

Proof: As the optimization problem $\mathbb{OP}$ is feasible at time step k, we get the optimal control sequence U^i_k and the corresponding sequence of state trajectories X^i_k, respectively,discussed Lemma 1. Since $\mathbb{OP}$ is feasible at time step k, it follows from Lemma 1 that an optimal control sequence U^i_{k+1} also exists for the next time step $k+1$. However, since the optimal control sequence U^i_{k+1} is not known exactly, we consider a sub-optimal control sequence $\widetilde{U}^i_{k+1}$ as in (13). Let the corresponding state trajectories be $\widetilde{X}^i_{k+1}$ and the corresponding cost function would be $\widetilde{J}^i_{k+1}$. Since $\widetilde{U}^i_{k+1}$ is not optimal, we have: $\widetilde{J}^i_{k+1} \ge J^i_{k+1}$. The cost function $\widetilde{J}^i_{k+1}$ can be expressed as follows:

$$\widetilde{J}^i_{k+1} = \|x^i_{N+1|k} - x^i_{ref}\|^2_P + \sum_{j=1}^{N}\left\{\|x^i_{j|k} - x^i_{ref}\|^2_Q + \|u^i_{j|k} - u^i_{ref}\|^2_R\right\}. \quad (15)$$

Now subtracting (15) from (12a), we obtain:

$$\widetilde{J}^i_{k+1} - J^i_k = \|A_d x^i_{N|k} + B_d u^i_{N|k} - x^i_{ref}\|^2_P + \|x^i_{N|k} - x^i_{ref}\|^2_Q + \|u^i_{N|k} - u^i_{ref}\|^2_R - \|x^i_{N|k} - x^i_{ref}\|^2_P - \|x^i_{0|k} - x^i_{ref}\|^2_Q - \|u^i_{0|k} - u^i_{ref}\|^2_R. \quad (16)$$

Note that $u^i_{N|k} = u^i_{N-1|k+1} = u^i_{ref} + K(x^i_{N|k} - x^i_{ref})$, and according to (5): $(A_d - I_n)x^i_{ref} + B_d u^i_{ref} = 0$. Using these relations in (16), following relation is obtained:

$$\widetilde{J}^i_{k+1} - J^i_k = (x^i_{N|k} - x^i_{ref})^{\mathsf{T}}[(A_d + B_d K)^{\mathsf{T}} P (A_d + B_d K) - P + Q + K^{\mathsf{T}} R K](x^i_{N|k} - x^i_{ref}) - \Big[\|x^i_{0|k} - x^i_{ref}\|^2_Q + \|u^i_{0|k} - u^i_{ref}\|^2_R\Big]. \quad (17)$$

The term, $(\|x^i_{0|k} - x^i_{ref}\|^2_Q + \|u^i_{0|k} - u^i_{ref}|^2_R) > 0$. Further, since (14) holds, it follows from (17) that: $\tilde{J}^i_{k+1} - J^i_k < 0$. Further, since $\tilde{J}^i_{k+1} \geq J^i_{k+1}$, we have: $J^i_{k+1} < J^i_k$. Hence, the cost function J^i_k decreases at each iteration. ■

According to Lemma 2, the cost function converges J^i_k as the time step advances if the matrix inequality (14) holds. Note that in (14), the matrices P and K are variables, and they are the design parameters. We will now formulate a linear matrix inequality (LMI) optimization to compute P and K. Note that Lemma 2 is also true when the equality holds for (14). In such case, one may compute P and K by solving an LQR problem. Consider two matrices L and M such that $L = P^{-1}$ and $M = KL$. Then, multiply (14) from left and right with L, which yields the following matrix inequality:

$$(LA_d^\mathsf{T} + M^\mathsf{T}B_d^\mathsf{T})L^{-1}(A_dL + B_dM) - L + L^\mathsf{T}QL \\ + M^\mathsf{T}RM \preceq 0. \quad (18)$$

Using (18), we formulate the following LMI optimization to compute P and K.

$$\min_{L,M} \quad -\operatorname{logdet}(L) \quad \text{such that}$$
$$\begin{bmatrix} L & LA_d^\mathsf{T}+M^\mathsf{T}B_d^\mathsf{T} & LQ^{\frac{1}{2}} & R^{\frac{1}{2}}M^\mathsf{T} \\ A_dL+B_dM & L & \mathbf{0} & \mathbf{0} \\ Q^{\frac{1}{2}}L & \mathbf{0} & I_3 & \mathbf{0} \\ R^{\frac{1}{2}}M & \mathbf{0} & \mathbf{0} & I_1 \end{bmatrix} \succeq 0. \quad (19)$$

One may use LMI solvers, such as YALMIP [22] to solve the above LMI optimization. Once the above LMI optimization is solved, we obtain the matrices $P = L^{-1}$ and $K = ML^{-1}$.

The overall implementation of the control scheme for CAV is summarized in Algorithm 3.

Algorithm 3 MPC algorithm for each AV

```
Offline: Compute $P$ and $K$ by solving (19).
Online:
1: Compute $v^i_{ref}$ using Algorithm 1 for each signalized junction.
2: for $k \geq 0$ do
3:     Compute $\mathcal{X}^i_{\mathcal{T}_k}$ using Algorithm 2.
4:     Run $\mathbb{OP}$ and generates a control sequence $U^i_k = \{u^i_{j|k}\}_{j=0}^{N-1}$.
5:     Consider the first element $u^i_{0|k}$ of $U^i_k$ and apply $u^i_{0|k}$ in (2)
       with initial state $x^i_{0|k}$, and get $x^i_{1|k}$.
6:     Share the updated state $x^i_{1|k}$ of $i^{th}$ AV with $(i+1)^{th}$ AV.
7:     $k \leftarrow k + 1$.
8: end for
```

III. Numerical Simulation

We consider a CAV system consisting of four AVs, which are moving in a line on a single-lane road. Let the dynamics of each AV be as in (2), where (considering $\eta_i = 0.55$ sec and $t_s = 0.2$ sec):

$$A_d = \begin{bmatrix} 1 & 0.2 & 0.0178 \\ 0 & 1 & 0.1677 \\ 0 & 0 & 0.6951 \end{bmatrix}, \; B_d = \begin{bmatrix} 0.0022 \\ 0.0323 \\ 0.3049 \end{bmatrix}$$

We also considered that the vehicles are crossing the 4 signalized junction. The initial states of AVs are considered as: $x^1_0 = [560 \;\; 12 \;\; 0]^\mathsf{T}$, $x^2_0 = [546 \;\; 15 \;\; -1.2]^\mathsf{T}$, $x^3_0 = [527 \;\; 13 \;\; 1]^\mathsf{T}$ and $x^4_0 = [515 \;\; 8 \;\; 3]^\mathsf{T}$. The state and input constraints for i^{th} AV are: $0 \leq v^i_k \leq 30$, $-5 \leq a^i_k \leq 8$, and $-8 \leq u^i_k \leq 6$, for $i = 1, 2, \cdots, 4$. It is considered that the static gap and the reaction time, as used in (4), are: $\gamma = 5$ m and $\rho = 0.5$ sec, respectively. Then, by choosing $Q = diag(10^{-9}, 10, 2)$, $W = 10$, and the prediction horizon $N = 45$, we follow the procedures given in Algorithm 3. In the offline design we computed: $P = \begin{bmatrix} 0.0005 & 0.0004 & 0.00009 \\ 0.0004 & 45.2104 & 8.5689 \\ 0.00009 & 8.5689 & 5.4187 \end{bmatrix}$ and $K = [-0.00003 \;\; -2.4547 \;\; -1.2195]$. It is observed that each AV requires at most 1.21 sec for each iteration in simulation, which includes computing the terminal set and MPC. The terminal sets of four AVs at the initial time step ($k = 0$) are shown in Fig. (2). Note that the constraints set (3) for each AV is fixed over all k, whereas the safe distance constraint (4) gets updated at each time step k. Hence, it is required to compute the terminal set $\mathcal{X}^i_{\mathcal{T}_k}$ at each time step k for each AV. The positions of each AV, passing through four signalized junctions, are depicted in Fig. (3). It can be observed that the AVs have adjusted their speed profiles so that they do not have to wait near the SJs. Further, Fig. (4) shows that the constraints on velocity, acceleration, and control input profile for each AV are also satisfied. Additionally, it can be observed from Fig. (5) that the safe distance among the vehicles is also maintained.

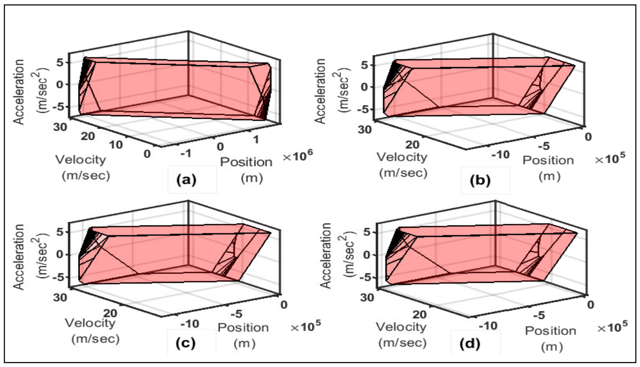

Fig. 2. Terminal sets of AVs at time step $k = 0$; (a) AV 1, (b) AV 2, (c) AV 3, (d) AV 4.

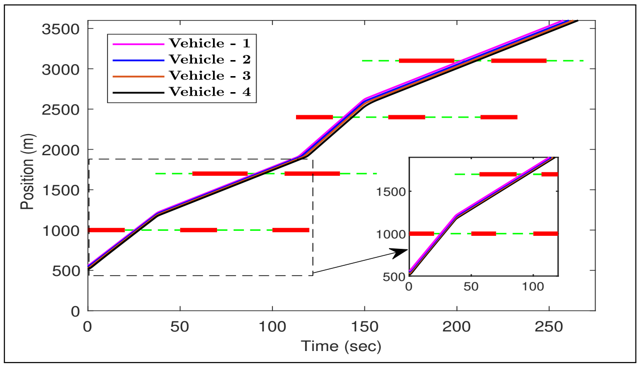

Fig. 3. Positions of AVs crossing four SJs. Red lines (solid) denote red signal duration, and green lines (dashed) denote green signal duration.

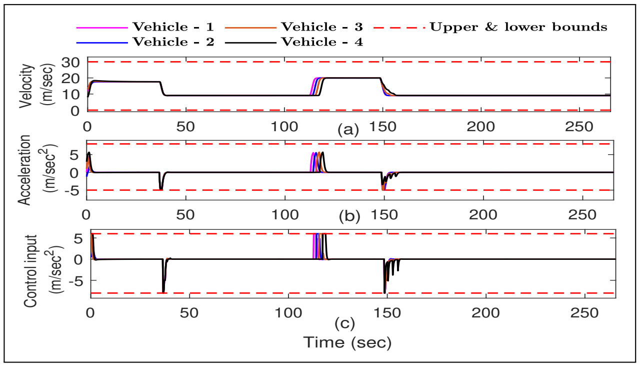

Fig. 4. (a) Velocity profile. (b) Acceleration. (c) Control input of each AV.

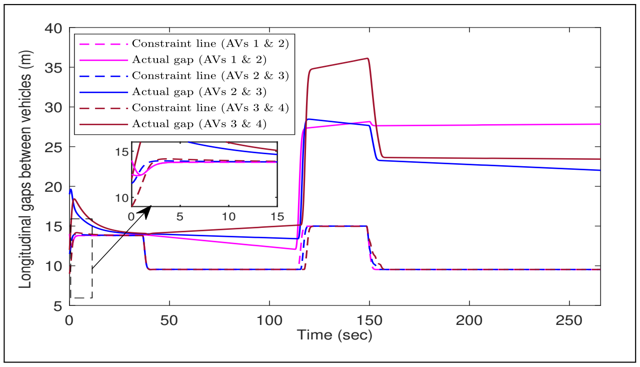

Fig. 5. Actual gap and gap constraint between two AVs on the road. The dashed lines (magenta, blue, brown) represent gap constraints between AVs 1 & 2, AVs 2 & 3, and AVs 3 & 4, respectively. The solid lines (magenta, blue, brown) represent the actual gap between AVs 1 & 2, AVs 2 & 3, and AVs 3 & 4, respectively.

IV. CONCLUSION

This work proposes a *velocity-guided control scheme* for a CAV system such that either none of the AVs wait at an SJ or only a limited number of vehicles get accumulated at an SJ when the red light is ON. For this, appropriate control signals for each AV are generated through the RHC approach in the MPC framework. An algorithm is proposed to generate reference velocities for the vehicles. Further, the inherent issues that arise in the MPC framework, such as recursive feasibility and stability analysis, are also investigated. To demonstrate the developed algorithms, numerical simulation is performed on a four vehicle CAV system, where satisfactory results are obtained. Note that in this work, we have considered an ideal scenario for roadway traffic, where real-world difficulties, such as vehicle dynamics uncertainties, communication uncertainties, and the intervention of human-driven vehicles, are not considered. It is expected that the uncertainties related issues can be addressed in the robust MPC framework. We are leaving these extensions as our future research work.

REFERENCES

[1] (2023) Tomtom traffic index website. [Online]. Available: https://www.tomtom.com/traffic-index/ranking/?country=IN

[2] K. Dresner and P. Stone, "A multiagent approach to autonomous intersection management," *Journal of artificial intelligence research*, vol. 31, pp. 591–656, 2008.

[3] C. Chen, Q. Xu, M. Cai, J. Wang, J. Wang, and K. Li, "Conflict-free cooperation method for connected and automated vehicles at unsignalized intersections: Graph-based modeling and optimality analysis," *IEEE Transactions on Intelligent Transportation Systems*, vol. 23, no. 11, pp. 21 897–21 914, 2022.

[4] B. Chalaki and A. A. Malikopoulos, "Optimal control of connected and automated vehicles at multiple adjacent intersections," *IEEE Transactions on Control Systems Technology*, vol. 30, no. 3, pp. 972–984, 2021.

[5] ——, "Time-optimal coordination for connected and automated vehicles at adjacent intersections," *IEEE Transactions on Intelligent Transportation Systems*, vol. 23, no. 8, pp. 13 330–13 345, 2021.

[6] R. Hult, M. Zanon, S. Gros, and P. Falcone, "Optimal coordination of automated vehicles at intersections: Theory and experiments," *IEEE Transactions on Control Systems Technology*, vol. 27, no. 6, pp. 2510–2525, 2019.

[7] R. Hult, M. Zanon, S. Gros, H. Wymeersch, and P. Falcone, "Optimisation-based coordination of connected, automated vehicles at intersections," *Vehicle System Dynamics*, vol. 58, no. 5, pp. 726–747, 2020.

[8] M. Kneissl, A. Molin, H. Esen, and S. Hirche, "A feasible mpc-based negotiation algorithm for automated intersection crossing," in *2018 european control conference (ecc)*. IEEE, 2018, pp. 1282–1288.

[9] M. A. S. Kamal, J.-i. Imura, T. Hayakawa, A. Ohata, and K. Aihara, "Smart driving of a vehicle using model predictive control for improving traffic flow," *IEEE Transactions on Intelligent Transportation Systems*, vol. 15, no. 2, pp. 878–888, 2014.

[10] H. Dong, W. Zhuang, B. Chen, Y. Lu, S. Liu, L. Xu, D. Pi, and G. Yin, "Predictive energy-efficient driving strategy design of connected electric vehicle among multiple signalized intersections," *Transportation Research Part C: Emerging Technologies*, vol. 137, p. 103595, 2022.

[11] C. Chen, J. Wang, Q. Xu, J. Wang, and K. Li, "Mixed platoon control of automated and human-driven vehicles at a signalized intersection: dynamical analysis and optimal control," *Transportation research part C: emerging technologies*, vol. 127, p. 103138, 2021.

[12] B. Asadi and A. Vahidi, "Predictive cruise control: Utilizing upcoming traffic signal information for improving fuel economy and reducing trip time," *IEEE transactions on control systems technology*, vol. 19, no. 3, pp. 707–714, 2010.

[13] B. HomChaudhuri, A. Vahidi, and P. Pisu, "Fast model predictive control-based fuel efficient control strategy for a group of connected vehicles in urban road conditions," *IEEE Transactions on Control Systems Technology*, vol. 25, no. 2, pp. 760–767, 2016.

[14] M. Hosseinzadeh, B. Sinopoli, I. Kolmanovsky, and S. Baruah, "Mpc-based emergency vehicle-centered multi-intersection traffic control," *IEEE Transactions on Control Systems Technology*, vol. 31, no. 1, pp. 166–178, 2023.

[15] H. Rastgoftar and J.-B. Jeannin, "A physics-based finite-state abstraction for traffic congestion control," in *2021 American Control Conference (ACC)*, 2021, pp. 237–242.

[16] A. Odekunle, W. Gao, C. Anayor, X. Wang, and Y. Chen, "Predictive cruise control of connected and autonomous vehicles: An adaptive dynamic programming approach," in *SoutheastCon 2018*. IEEE, 2018, pp. 1–6.

[17] J. Hu, P. Bhowmick, F. Arvin, A. Lanzon, and B. Lennox, "Cooperative control of heterogeneous connected vehicle platoons: An adaptive leader-following approach," *IEEE Robotics and Automation Letters*, vol. 5, no. 2, pp. 977–984, 2020.

[18] S. E. Sheikholeslam, *Control of a class of interconnected nonlinear dynamical systems: The platoon problem*. University of California, Berkeley, 1991.

[19] B. Wittenmark, K.-E. Årzén, and K. J. Åström, *Computer Control: An Overview*, ser. IFAC PROFESSIONAL BRIEF. International Federation of Automatic Control, 2002.

[20] F. Borrelli, A. Bemporad, and M. Morari, *Predictive control for linear and hybrid systems*. Cambridge University Press, 2017.

[21] M. Herceg, M. Kvasnica, C. N. Jones, and M. Morari, "Multi-parametric toolbox 3.0," in *2013 European control conference (ECC)*. IEEE, 2013, pp. 502–510.

[22] J. Löfberg, "Yalmip : A toolbox for modeling and optimization in matlab," in *In Proceedings of the CACSD Conference*, Taipei, Taiwan, 2004.